Molecular Therapy
Oncolytics
Original Article

AMERICAN SOCIETY of GENE & CELL THERAPY

Insertion of the Type-I IFN Decoy Receptor B18R in a miRNA-Tagged Semliki Forest Virus Improves Oncolytic Capacity but Results in Neurotoxicity

Tina Sarén,[1] Mohanraj Ramachandran,[1] Miika Martikainen,[1] and Di Yu[1]

[1]Department of Immunology, Genetics, and Pathology, Science for Life Laboratory, Uppsala University, Uppsala, Sweden

Oncolytic Semliki Forest virus (SFV) has been suggested as a potential candidate for the treatment of glioblastoma and neuroblastoma. However, the oncolytic capacity of SFV is restricted by the anti-viral type-I interferon (IFN) response. The aim of this study was to increase the oncolytic capacity of a microRNA target tagged SFV against glioblastoma by arming it with the Vaccinia-virus-encoded type-I IFN decoy receptor B18R (SFV4B18RmiRT) to neutralize type-I IFN response. Expression of B18R by SFV4B18RmiRT aided neutralization of IFN-β, which was shown by reduced STAT-1 phosphorylation and improved virus spread in plaque assays. B18R expression by SFV4 increased its oncolytic capacity in vitro against murine glioblastoma (CT-2A), regardless of the presence of exogenous IFN-β. Both SFV4B18RmiRT and SFV4miRT treatments controlled tumor growth in mice with syngeneic orthotopic gliomablastoma (CT-2A). However, treatment with SFV4B18RmiRT induced severe neurological symptoms in some mice because of virus replication in the healthy brain. Neither neurotoxicity nor virus replication in the brain was observed when SFV4miRT was administered. In summary, our results indicate that the oncolytic capacity of SFV4 was improved in vitro and in vivo by incorporation of B18R, but neurotoxicity of the virus was increased, possibly due to loss of microRNA targets.

INTRODUCTION

The most common type of primary brain tumors are gliomas, which are classified according to the World Health Organization (WHO) as grade I–IV, where III/IV are malignant.[1,2] Grade IV, also called glioblastoma, is the most malignant glioma; it accounts for more than half of the cases and only 5% of patients live 5 years after glioblastoma diagnosis.[3] The current treatments for glioblastoma consist of surgical tumor resection in many cases, followed by external beam irradiation and temozolomide. Despite this aggressive treatment regimen, patients experience tumor relapse.[1]

Oncolytic viruses (OVs) can specifically target and kill tumor cells and leave healthy cells unharmed.[4] Semliki Forest virus (SFV) is an enveloped positive single-strand RNA virus of the *Togaviridae* family.[5] SFV has natural ability to home to the CNS upon systemic delivery in mice and hence has gained interest as an OV for the treatment of glioblastoma.[6–8] There are several strains of SFV, and the virulence of an individual strain is determined depending on the pathogenesis in adult mice. SFV4 is neurovirulent, causing severe encephalitis in adult mice, whereas A7(74) is an avirulent strain.[5] VA7 is a vector derived from A7(74) that has shown promise in an immunodeficient glioma model.[7] In immunocompetent models, however, VA7 failed due to its sensitivity to type-I interferons (IFNs).[9,10] Recently, the neurotoxic SFV4 strain has gained interest as an oncolytic agent because it is less sensitive to type-I IFN. Others and we have inserted CNS-related microRNA (miRNA) targets into the SFV4 genome to prevent neurotoxicity and encephalitis in mice.[6,8,11] However, therapeutic efficacy of the miRNA-detargeted SFV4 (SFV4miRT) still negatively correlates with the type-I IFN anti-viral response.[8] Upon viral infection, cells secrete IFN-β, which acts in an autocrine and paracrine manner to induce an anti-viral state in virus-infected and neighboring cells. IFN-β binds to the interferon-α/β receptor (IFNAR)[12] and induces phosphorylation of STAT (signal transducer and activator of transcription) 1 and 2 proteins. The phosphorylated STAT proteins, together with IRF9 (IFN-regulatory factor 9), form the transcription factor ISG3 (IFN-stimulated gene factor 3), which initiates expression of interferon-stimulated genes (ISGs) that both directly and indirectly prevent virus propagation.[13]

The *B18R* gene in the vaccinia virus (VV) genome encodes for a decoy receptor, which binds to type-I IFN. The B18R protein is secreted from cells infected with VV and acts both as a soluble and a membrane-associated receptor that neutralizes the anti-viral effects of type-I IFN.[14–16] Cells are thereby kept in a state where they are susceptible to viral infection. Administration of VV can synergistically enhance the antitumor activity of vesicular stomatitis virus, a type-I IFN-sensitive RNA virus, and this is dependent on the activity of the VV *B18R* gene product.[17] Here, we have incorporated *B18R* into a previously described SFV4miRT[8] to improve its oncolytic efficacy against type-I IFN-responsive

Received 15 June 2017; accepted 2 October 2017;
https://doi.org/10.1016/j.omto.2017.10.001.

Correspondence: Di Yu, Department of Immunology, Genetics, and Pathology, Uppsala University, 75185 Uppsala, Sweden.
E-mail: di.yu@igp.uu.se

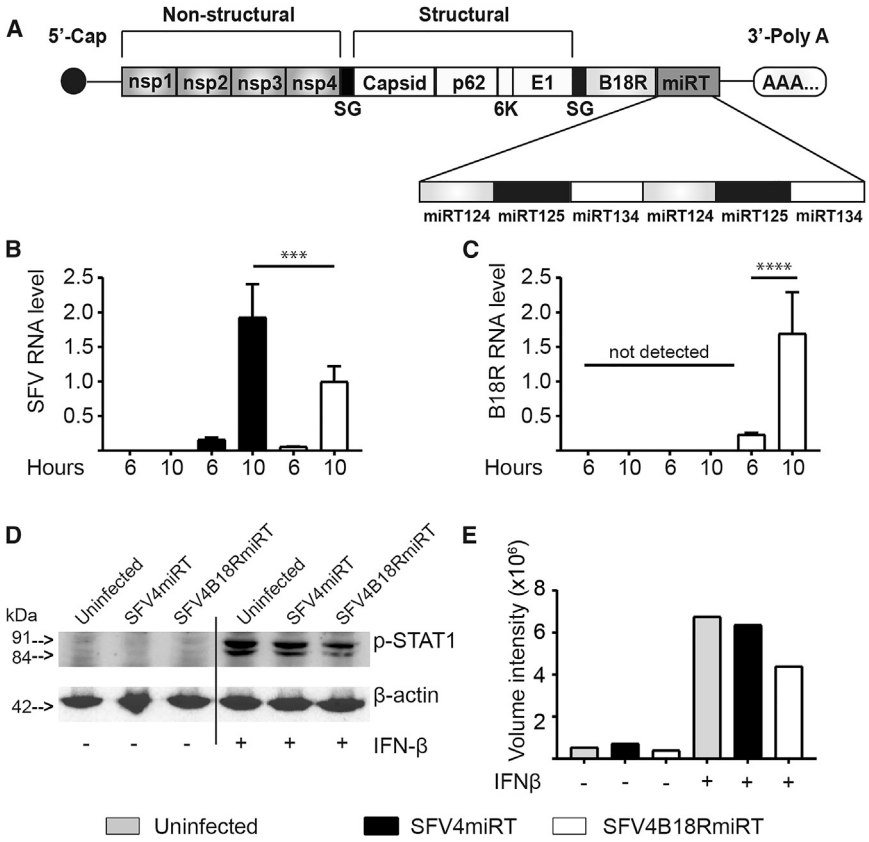

Figure 1. Functional Analysis of B18R Expressed by SFV4B18RmiRT

(A) Schematic representation of the SFV construct. B18R was inserted downstream of the structural genes under the control of a subgenomic promoter (SG). Target sequences for miR-124, miR-125 and miR-134 (in duplicates) were inserted in the 3′ UTR. (B and C) CT-2A cells were infected (MOI 10) with SFV4miRT or SFV4B18RmiRT, and RNA was extracted from infected cells after 6 and 10 hr. Uninfected cells were used as controls. Real-time PCR was used to determine SFV nsP3 (B) and B18R (C) RNA levels. RNA levels were normalized toward GAPDH. Values are shown as mean ± SEM and were compared by one-way ANOVA with Sidak post hoc test (n = 3, ****p < 0.0001, ***p < 0.001). (D) Western blot for detection of p-STAT1 (Tyr701) in CT-2A cells. Supernatants were collected from BHK21 cells infected (MOI 10) with SFV4miRT or SFV4B18RmiRT overnight. Exogenous mIFN-β (200 pg/mL) was added to the supernatant for 60 min to allow for B18R in the SFV4B18RmiRT supernatant to neutralize IFN-β. Supernatants were then added to CT-2A cells for 30 min, after which p-STAT1 was detected using western blot to determine IFN-β activity and thereby indirect B18R neutralizing capacity. (E) Quantification of p-STAT1 (both isoforms) from 1 day presented as volume intensity normalized to β-actin. The blot was analyzed in ImageLab software.

glioblastomas. We investigated the ability of B18R to neutralize IFN-β responses and how it affected the oncolytic capacity of the virus in vitro and in vivo. We also performed a safety assessment in vivo to determine if insertion of B18R altered the toxicity of the miRNA-targeted virus.

RESULTS

Construction of SFV4B18RmiRT and Validation of Functional B18R Protein Expression

To prevent neurovirulence of SFV4, the VV *B18R* gene was inserted into an SFV4 vector containing target sequences against miR-124, miR-125, and miR-134, which are present in healthy cells in the murine CNS.[8] The virus is hereafter referred to as SFV4B18RmiRT (Figure 1A). Because no commercial antibody is available to detect B18R, we examined B18R expression at its transcriptional level. RNA from murine glioblastoma cells (CT-2A) infected with SFV4miRT or SFV4B18RmiRT at a MOI of 1 were harvested 6 or 10 hr post infection (p.i.) to evaluate viral replication and transgene expression. SFV (nsP3) RNA was detected in CT-2A cells infected with both SFV4miRT and SFV4B18RmiRT, and the amount of RNA increased with time, suggesting active viral replication (Figure 1B). However, SFV4B18RmiRT-infected cells had significantly lower amounts of SFV RNA, 10 hr p.i., than those infected with SFV4miRT, indicating that insertion of the *B18R* transgene may decrease the rate of viral replication (Figure 1B). As expected, B18R RNA was only detected in SFV4B18RmiRT-infected cells and its RNA levels increased over time (Figure 1C).

The presence of functional B18R protein in the supernatant from virus-infected BHK21 cells was also analyzed by determining the IFN-β neutralizing capacity. Supernatant was incubated with exogenous IFN-β to allow for B18R to bind and neutralize IFN-β and then the mixture was added to CT-2A cells to determine STAT1 phosphorylation (p-STAT1), which is a downstream event in the IFN-β signaling pathway. Supernatant collected from SFV4B18RmiRT-infected cells and mixed with exogenous IFN-β induced lower p-STAT1 than that collected from SFV4miRT-infected cells, indicating an IFN-β neutralizing capacity of B18R (Figures 1D and 1E). Supernatant collected from SFV4miRT-transduced BHK21 cells could not neutralize exogenous IFN-β and resulted in similar levels of p-STAT1 induction as for the supernatant collected from uninfected BHK21 cells (Figures 1D and 1E).

Insertion of B18R Increases Oncolytic Capacity and Spread In Vitro

The oncolytic capacity of SFV4miRT and SFV4B18RmiRT against murine glioblastoma and neuroblastoma was compared in vitro. Cells were infected at MOIs ranging from 0.01 to 10 PFU/cell in the absence (Figures 2A, 2C, and 2E) or presence (Figures 2B, 2D, and 2F) of

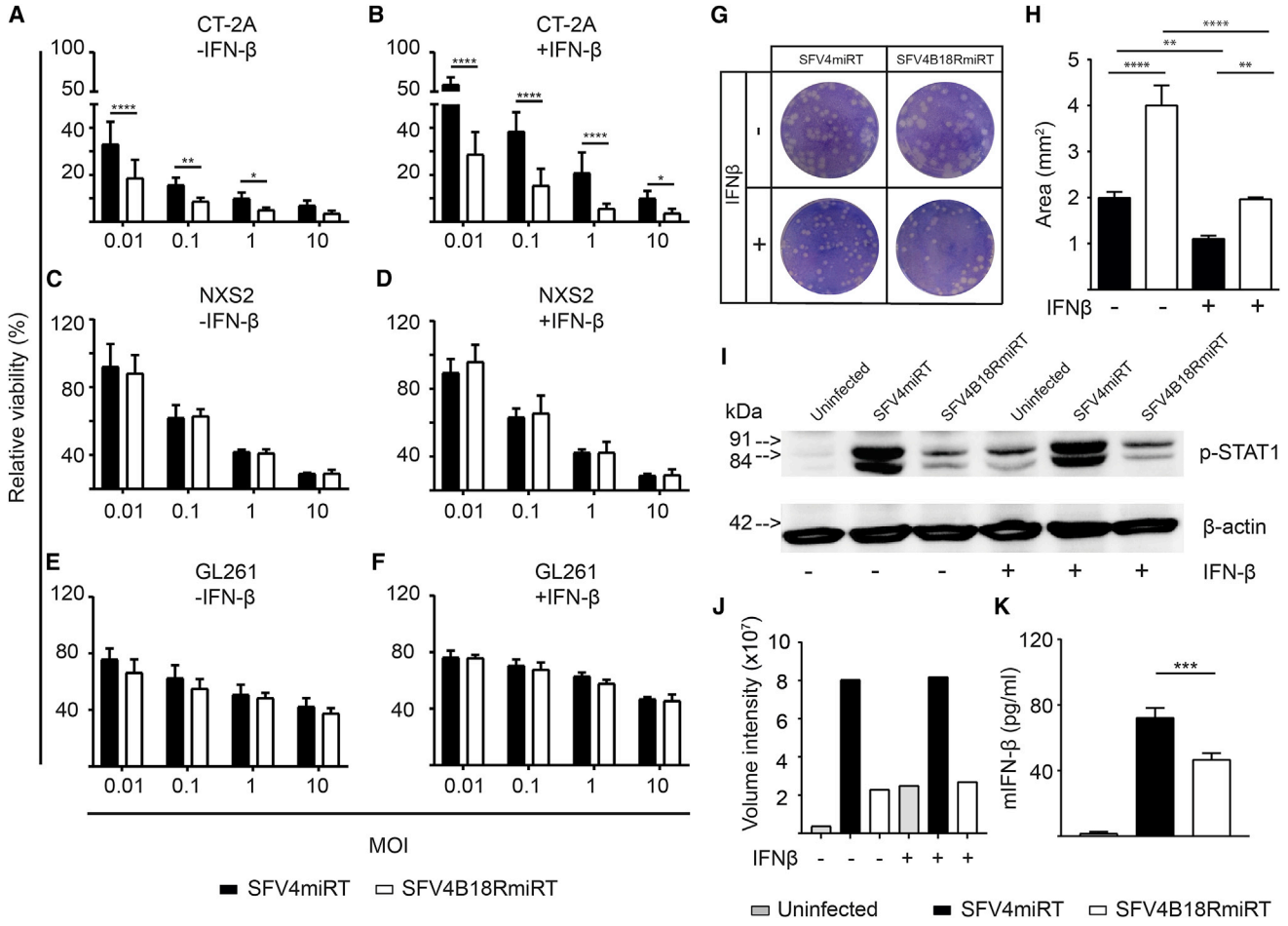

Figure 2. Presence of B18R Increases Oncolytic SFV Capacity and Viral Spread In Vitro

(A–F) The ability of SFV4miRT and SFV4B18RmiRT to kill CT-2A (A and B), NXS2 (C and D), and GL261 (E and F) cells was assessed in the absence (A, C, and E) or presence (B, D, and F) of exogenous mIFN-β (10 pg/mL). Cells were infected with an MOI gradient ranging from 0.01 to 10, and cell viability was determined using the alamarBlue assay 48 or 72 hr after infection. The experiment was repeated at least twice with internal triplicates. Values are shown as mean ± SEM and were compared by two-way ANOVA with Holm-Sidak post hoc test (****$p < 0.0001$, **$p < 0.01$, *$p < 0.05$). (G and H) Viral spread was assessed in a plaque assay by infecting NXS2 cells at MOI 0.005 with or without exogenous mIFN-β (10 pg/mL). Plaques were detected using crystal violet 3 days p.i. (G), and the size (mm^2) was determined using ImageJ. Values are shown as mean ± SEM (H) and were compared by one-way ANOVA with Tukey post hoc test (****$p < 0.0001$, **$p < 0.01$). (I and J) The amount of p-STAT1 (Tyr701) in CT-2A cells upon SFV4miRT or SFV4B18RmiRT infection was determined using western blot (I) and quantified (J). CT-2A cells were infected at MOI 10 for 6 hr and left untreated or treated with mIFN-β (50 pg/mL) for 30 min. One representative blot is shown from duplicate experiments. (J) Quantification of p-STAT1 (both isoforms) presented as volume intensity normalized to β-actin. The blots were analyzed in ImageLab. (K) mIFN-β quantification in the supernatant of CT-2A cells infected with SFV4miRT or SFV4B18RmiRT at MOI 10 after overnight incubation using ELISA. The experiment was repeated at least two times with internal duplicates. Means were compared by one-way ANOVA with Tukey post hoc test (***$p < 0.001$).

exogenous IFN-β (10 pg/mL). SFV4B18RmiRT had a significantly increased oncolytic capacity in CT-2A cells when compared to SFV4miRT independent of exogenous IFN-β (Figures 2A and 2B). NXS2 cells were sensitive to both viruses, and no difference in oncolytic capacity was observed (Figures 2C and 2D). However, when a higher amount of IFN-β was added, SFV4B18RmiRT had a significant increase in oncolytic capacity against murine neuroblastoma (NXS2) cells compared to SFV4miRT at MOI 0.1 and 1 (Figure S1). GL261 cells were resistant to both viruses independent of exogenous IFN-β (Figures 2E and 2F).

A plaque assay was carried out to test our hypothesis that B18R, by neutralizing the anti-viral effects of IFN-β, can increase the ability of SFV4B18RmiRT to infect neighboring cells and spread. NXS2 cells were infected with SFV4miRT or SFV4B18RmiRT, with or without addition of exogenous IFN-β. SFV4B18RmiRT generated bigger plaques than did SFV4miRT, both in the presence and absence of exogenous IFN-β, indicating that B18R increases SFV spread to neighboring cells. However, spread of both viruses was still negatively affected by exogenous IFN-β (Figures 2G and 2H), indicating that IFN-β is an important factor in limiting SFV replication and spread.

To verify if the increased spread of SFV4B18RmiRT was through neutralization of IFN-β, STAT1 phosphorylation was studied in CT-2A cells upon virus infection. SFV4 infection of CT-2A cells is known to induce IFN-β secretion and subsequently induce STAT1 phosphorylation.[6] SFV4miRT induced stronger p-STAT1 compared to the uninfected control, regardless of whether exogenous IFN-β was added or not (Figures 2I and 2J). SFV4B18RmiRT infection induced lower amounts of p-STAT1 independent of exogenous IFN-β (Figures 2I and 2J). Both viruses induced IFN-β secretion in CT-2A cells upon infection (Figure 2K). These results indicate that B18R expressed from SFV4B18RmiRT-infected cells reduces the anti-viral effect of IFN-β on the tumor cells.

SFV4B18RmiRT and SFV4miRT Treatment Controls Tumor Growth in Glioma-Bearing Mice

C57BL/6NRj mice with orthotopically growing CT-2A/fLuc tumors were treated once intraperitoneally (i.p.) with either SFV4B18RmiRT or SFV4miRT (1×10^7 PFU/mice; 8 mice per group) to evaluate the therapeutic efficacy in vivo. PBS treatment (5 mice) was used as control. Tumor growth post treatment was monitored by bioluminescence imaging (Figure 3A, representative image), and tumor burden on days 3 and 7 post treatment was quantified as a fold increase in bioluminescence (Figure 3B). Treatment with both SFV4B18RmiRT and SFV4miRT viruses controlled CT-2A tumor growth 7 days p.i. compared to the PBS-treated mice (Figure 3B). Virus replication was also observed within the tumors harvested from mice administered with SFV4miRT (Figure 3C) and SFV4B18RmiRT (Figure 3D). Long-term survival post treatments was not analyzed because half the mice injected with SFV4B18RmiRT (4/8) were sacrificed at earlier time points due to virus-related neurotoxicity. This is discussed in the next section.

Insertion of *B18R* Increases Neurotoxicity of SFV4miRT

SFV4miRT has been confirmed safe upon systemic administration in adult mice,[8] and also, this time, none of the eight mice treated with SFV4miRT exhibited any neurological symptoms. However, four mice treated with SFV4B18RmiRT exhibited virus-related neurological symptoms at 6 days p.i. Symptoms were scored as 0 (no symptoms), 0.1 (mild symptom), or 0.3 (severe symptom or accumulation of mild symptoms). As mentioned above, none of the mice in the SFV4miRT group developed virus-related symptoms (Figure 3E) but were sacrificed later on due to tumor burden. Mice infected with SFV4B18RmiRT started to show mild symptoms, such as limping and weakness at day 4 after virus injection. On days 6 and 7 after viral injection, four mice (50%) had to be sacrificed due to severe neurological symptoms, including hind leg paralysis and hunching back. The remaining four mice injected with SFV4B18RmiRT did not develop virus-related symptoms (Figure 3F). Brains from sacrificed animals were excised for analysis. SFV proteins were not observed in the healthy brain of SFV4miRT-infected mice sacrificed at early (# to be used as a control, Figure 3G) or late (¤ sacrificed due to tumor burden, Figure 3H) time points after virus injection. Mice injected with SFV4B18RmiRT that were sacrificed due to virus-related neurological symptoms (*, Figure 3I) showed strong staining for viral proteins in healthy brain tissue. In contrast, long-term surviving mice from the SFV4B18RmiRT group that did not develop virus-related symptoms (but that were sacrificed due to tumor burden) had no viral staining in healthy brain tissue (¤, Figure 3J).

We hypothesized that the neurotoxicity of SFVB18RmiRT was caused by the loss of the miRT cassette due to viral genome instability upon insertion of a large transgene (B18R). To assess this, an in vitro qPCR assay was carried out to detect the presence of nsP3, miRT cassette, and B18R transgene (Figures 3K and 3L). RNA from CT-2A cells infected in vitro with SFV4miRT or SFVB18RmiRT were analyzed 6 and 10 hr p.i. The amount of miRT RNA (miRT region) in relation to that of SFV RNA (nsP3 region) in SFV4miRT-infected cells was equal or, in fact, higher (Figure 3K). This is because miRT expression is under the control of the second subgenomic promoter, which produces more copies of the mRNA than in the nsP region. Cells infected with SFV4B18RmiRT, on the other hand, had lower levels of miRTs than the nsP3 region (Figure 3K), indicating loss of miRTs from the viral genome. Levels of B18R RNA, which is also under the control of the second subgenomic promoter, is higher than the amount of SFV RNA in SFV4B18RmiRT-infected cells, further indicating loss of the miRT cassette when the B18R gene is present (Figure 3L).

DISCUSSION

Pre-clinically, OVs have shown great promise against malignant glioma. SFV is an interesting candidate for the treatment of glioblastoma due to its ability to target the brain upon systemic delivery and to kill glioblastoma cells.[6–8] Type-I IFN-mediated anti-viral immune response is a restricting factor for the oncolytic efficacy of SFV,[9] although it is important to elicit a strong dendritic cell -dependent anti-tumor immunity.[18] To overcome type-I IFN response and improve oncolytic efficacy, SFV has been co-administered with VV and expression of B18R by VV decreased the negative effect of type-I IFN on SFV. This has been proposed to be due to neutralization of type-I IFN by a decoy receptor, B18R, expressed by VV.[19] In the current work, we inserted the *B18R* encoding gene into the SFV4 genome to create a single OV to overcome the antiviral immune responses and thereby improve the oncolytic efficacy of SFV4. Cells infected with SFV4B18RmiRT expressed B18R, but insertion of *B18R* slowed down the virus replication (Figures 1B and 1C). This is consistent with previous findings that insertion of the transgene for EGFP into the SFV4 genome decreased viral replication compared to the wild-type virus.[20] We could also show that the expressed B18R was functional because B18R containing supernatant decreased the activity of exogenously added IFN-β (Figures 1D and 1E).

Our results indicate an improved killing capacity of SFV4B18RmiRT against CT-2A cells in vitro (Figures 2A and 2B) but not against NXS2 and GL261 cells (Figures 2C–2F). It is known that GL261 cells are highly resistant to SFV4 oncolysis due to both high secretion and responsiveness to IFN-β.[8,9] CT-2A cells, on the other hand, secrete less IFN-β, which makes it more susceptible to SFV oncolysis,[8] and even more susceptible to SFV4B18RmiRT (Figures 2A and 2B).

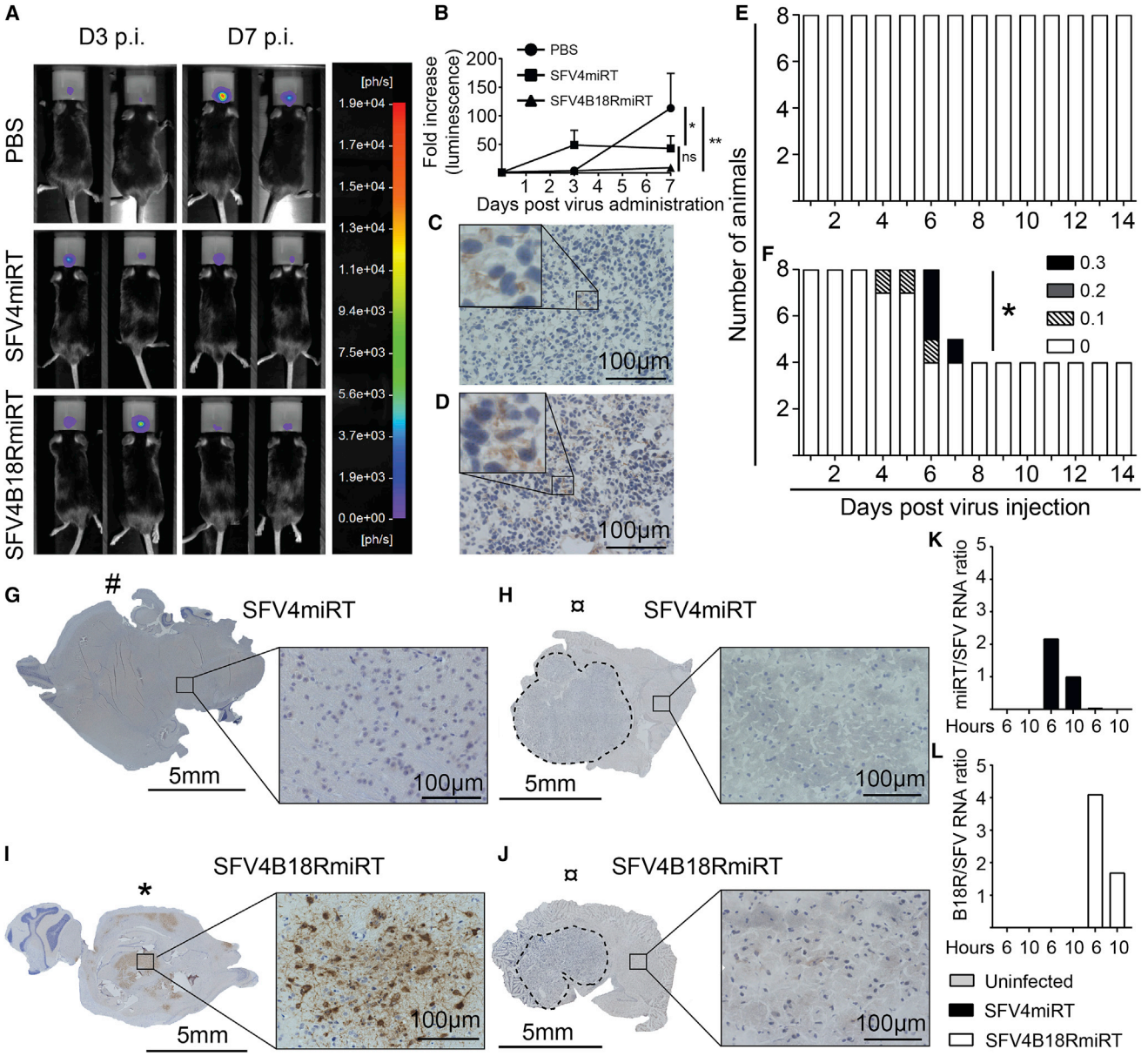

Figure 3. Therapeutic Efficacy and Neurotoxicity of SFV4B18RmiRT

To determine the therapeutic efficacy of SFV4B18RmiRT in vivo, CT-2A/fLuc cells were injected orthotopically in the brain of C57BL/6NRj mice. 11 days later, when tumors were visible by in vivo bioluminescence imaging, mice were injected (i.p.) either with PBS (n = 5), SFV4miRT (n = 8), or SFV4B18RmiRT (n = 8) at 1×10^7 PFU. (A) Representative pictures of mice with CT-2A/fLuc tumors 3 and 7 days after virus administration. (B) Quantification of tumor growth (fold increase in luminescence) after virus administration (PBS n = 5, SFV4miRT n = 8, and SFV4B18RmiRT n = 5). Values are shown as mean ± SEM and were compared by two-way ANOVA with Tukey post hoc test (**$p < 0.01$; *$p < 0.05$; not significant [n.s.], $p > 0.05$). (C and D) Immunohistochemical staining for SFV proteins in the tumor area in a mice brain injected with SFV4miRT (C) or SFV4B18RmiRT (D) (optical magnification 40X, inset 4x digital magnification). (E and F) Scoring of neurological symptoms in mice injected with SFV4miRT (n = 8) (E) or SFV4B18RmiRT (n = 8) (F). The symptoms were scored in a scale ranging from 0 (no symptoms) to 0.3 (severe or accumulation of several mild symptoms). When reaching a score of 0.3, mice were sacrificed. (G–J) Brains were excised from virus-injected mice and stained for SFV proteins in the non-tumor area of the brain in mice injected with SFV4miRT that were sacrificed early (#, control) (G) or late (H) due to tumor burden (¤) and mice injected with SFV4B18RmiRT sacrificed early (I) due to virus-related symptoms (*) or late (J) due to tumor burden (¤). (K and L) SFV (nsp), B18R, and miRT RNA levels in SFV4miRT- and SFVB18RmiRT-infected CT-2A cells were determined by qPCR. Cells were infected at MOI 10, and RNA was extracted 6 and 10 hr p.i. RNA levels were normalized toward GAPDH. miRT (K) and B18R (L) expression level was related to viral replication (SFV RNA level). #, sacrificed as control; *, sacrificed due to virus-related symptoms (neurotoxicity); ¤, sacrificed due to tumor burden.

NXS2 cells were sensitive to SFV oncolysis but no difference between the viruses with or without *B18R* was observed (Figure 2C), most likely because NXS2 cells do not secrete IFN-β.[8] Also, no difference in oncolytic capacity against NXS2 was observed in the presence of exogenous IFN-β (10 pg/mL) (Figure 2D). However, when a higher amount of IFN-β was added, SFV4B18RmiRT had a significantly higher oncolytic capacity compared to SFV4miRT at higher MOIs (Figure S1). These results indicate that NXS2 cells are responding to IFN-β but are less sensitive to type-I IFN than CT-2A and GL261 cells and thus require a higher dose to be protected. These results are consistent with a previous report.[8]

Upon viral infection, cells secrete type-I IFN that binds to the receptor of infected and surrounding cells and this will result in an anti-viral state, preventing viral replication and spread.[12] We could confirm that IFN-β was an important factor restricting SFV spread because plaque size decreased in cells infected with both viruses in the presence of exogenous IFN-β (Figures 2G and 2H). However, insertion of B18R could increase the ability of SFV to spread to neighboring cells (Figures 2G and 2H). Supporting this finding, others have reported that addition of VV increased the ability of SFV to spread due to B18R.[19] Furthermore, in another study B18R could increase spread of VSV, either when incorporated into the virus[21] or when produced by *E. coli*.[22] It is worth noting that NXS2 cells respond to IFN-β, but no secretion upon viral infection has been detected.[8] This does not exclude that small amounts of IFNs, undetectable in suspension, have an effect under restricted conditions. SFV4B18RmiRT induced less STAT1 phosphorylation compared to SFV4miRT (Figures 2I and 2J), further indicating an IFN-β-neutralizing capacity of B18R expressed by SFV. However, it needs to be taken into account that less IFN-β was detected following SFV4B18RmiRT infection (Figure 2K). This might be due to the reduced replication rate of SFV4B18RmiRT compared to SFV4miRT because it is known that the amount of type-I IFN secreted is proportional to the virus replication.[23] Another reason might be that the binding of B18R to IFN-β impaired its detection by ELISA. In combination with the results in which exogenous IFN-β was present, the results indicate that expression of the decoy receptor B18R by SFV4B18RmiRT increased its ability to spread to neighboring cells by binding to and neutralizing IFN-β and thereby preventing neighboring cells to enter an anti-viral state.

Both SFV4B18RmiRT and SFV4miRT treatments resulted in controlled tumor growth in mice bearing CT-2A gliomas when compared to the PBS treatment (Figure 3B). However, we did not observe a significant difference in tumor growth between the groups treated with different viruses even though there was a trend that SFV4B18RmiRT-treated mice had lower tumor burden compared to SFV4miRT-treated mice. This has also been previously reported when an oncolytic HSV was engineered to express B18R[24] and in another study in which co-administration of B18R producing *E. coli* together with VSV reduced tumor growth compared to virus or *E. coli* alone.[22] Day 7 p.i. bioluminescence imaging and tumor growth measurements were terminated because four mice from the SFV4B18RmiRT group developed virus-related neurological symptoms and had to be sacrificed (Figure 3F). Viral protein could be detected in tumors from virus-treated mice (Figures 3C and 3D). This is in accordance with confirmed previous findings that SFV4 can target the brain upon systemic delivery and replicate in a glioma tumor.[6,8]

Systemic administration of SFV4miRT, including targets for miR-124, miR-125, and miR-134, was safe (Figure 3E) and no virus proteins were detected in the healthy brain (Figures 3G and 3H). Some mice injected with SFV4B18RmiRT, on the other hand, developed severe neurological symptoms due to virus replication in the healthy brain (Figure 3I). Toxicity has been reported previously using SFV4 with targets for miR-124 and symptoms could be correlated to virus replication in the healthy brain, indicating sporadic escape.[11] It was shown that some viral clones lost either a few or, in one case, all miRTs.[11] In vitro, we observed a very low ratio of miRTs compared to SFV RNA, indicating a partial loss of the targets already in vitro (Figure 3K). We also tried to detect the miRT cassette in vivo without success (Figure S2). Moreover, we observed virus replication in the healthy brain of an SFV4B18RmiRT-injected mouse that was sacrificed due to virus-related symptoms (Figure 3I). This indicates loss of miRTs, which enables the virus to replicate in healthy cells. We speculate that insertion of B18R increased the instability of the virus genome and thereby the likelihood of losing the protective miRTs, explaining the severe symptoms observed.

In conclusion, incorporation of B18R increased the oncolytic capacity and spread of SFV4miRT in vitro through neutralizing effects of type-I IFN. However, SFV4B18RmiRT induced neurotoxicity in mice due to virus replication in the brain. In the future, to prevent neurotoxicity, the site of miRTs and also the transgene need to be optimized to increase stability of the viral genome.

MATERIALS AND METHODS

Cell Lines and Culturing Conditions

The murine glioblastoma cell line GL261 (kind gift from Dr. Geza, National Research Institute for Radiobiology and Radiohygiene, Safrany, Hungary) and the murine neuroblastoma cell line NXS2 (kind gift from Dr. Holger N. Lode, University of Greifswald, Germany) were cultured in DMEM Glutamax supplemented with 10% fetal bovine serum (FBS), 1% penicillin/streptomycin (PEST), and 1% sodium pyruvate. The murine glioblastoma cell line CT-2A (generously provided by Thomas Seyfried, Boston College) and Firefly-luciferase-expressing CT-2A-Fluc clones (generated by Jan Brun and David Stojdl, Children's Hospital of Eastern Ontario, Ottawa, Canada) were cultured in RPMI-1640 complemented with 10% FBS, 1% PEST, and 1% sodium pyruvate. BHK21 cells (kind gift from Andres Merits, University of Tartu) were cultured in GMEM (Glasgow's Modified Eagle Medium) supplemented with 10% FBS, 2% TPB (Tryptose Phosphate Broth, Teknova), 2% 1M HEPES, and 1% PEST. For transducing SFV in BHK21 cells, infectious GMEM medium supplemented with 1% PEST, 2% 1M HEPES,

and 10% FBS was used. All cell culture reagents were from Thermo Fisher Scientific (Waltham, MA) if nothing else is stated.

Virus Production

All cloning was performed in SFV4miRT, as previously described.[8] B18R was PCR amplified together with a subgenomic promoter using primers (5′-TGGTTGTGGTCACTTGCATTGGGCTCCGCA GATAAGGGCTGAGAGGACCTGTTATACACCTCTACGGCGGT CCTAGATTGGTGCGTTAATACACCCGGGCCACCCCATGATG AAAATGATGGTACATATATATTTCGTATCAT-3′ and 5′-CCA CATCGCGTCTCTGATCCTCACCTCGAGCGCCAGAATGCGTT CTTACTCCAATACTACTGTAGTTGTAAGGGTTTT-3′) that allowed Gibson assembly into the cloning vector pCMV-SFV4-2SG-nanoLuc-miR. Gibson assembly was performed according to the manufacturer's protocol (New England Biolabs, Ipswich, MA). B18R was inserted downstream of the structural genes in the viral genome before the miRTs and the resulting plasmid was named pCMV-SFV4-2SG-VVWB18R-miRT.

Infectious SFV4B18RmiRT virus particles were produced by electroporation of BHK21 cells with the pCMV-SFV4-2SG-VVWB18R-miRT plasmid. In short, BHK21 (5×10^6) cells were electroporated (at 200 V and 100 μF) with 5 μg SFV plasmid, along with 50 μg salmon sperm DNA (Thermo Fisher Scientific). Cells were seeded in a 10-cm culture dish with fresh culture medium. After 48 hr, the p0 virus stock was harvested and 100 μL p0 stock was added to a confluent 10-cm dish of BHK21 cells to produce the p1 stock, which was harvested 24 hr later. The p1 stock was concentrated on a 20% sucrose cushion for 3 hr at 25,000 rpm. Virus was titrated on BHK21 cells as plaque forming units (pfu).

PCR

SFV (nsP3), B18R, and miRT expression in vitro was assessed by infecting 5×10^5 CT-2A cells with SFV4miRT or SFV4B18RmiRT at MOI 1. Infected and uninfected cells were harvested 6 or 10 hr p.i. Total RNA was extracted using RNeasy mini kit (QIAGEN, Hilden, Germany) and cDNA was synthesized (iScript cDNA synthesis, Bio-Rad, Hercules, CA). Viral RNA levels were quantified by qPCR (IQ SYBR Green Supermix, Bio-Rad) using the following primers:

SFV 5′-TAATTCAAGCAGCGGAGCCA-3′ and 5′-TCTAGAACCG GGTCTCCTGG-3′; B18R 5′-GAGAGCCATTCAGCGCAAAG-3′ and 5′-CGGTGCACAAATACCTACGG-3′; miRT 5′-GATGTGGC ATTCACCGCGTGCCTTACGA-3′ and 5′-CTCAGGATCCTGTGA CTGGTTGACCAGAGGGAGTCC-3′; and GAPDH 5′- GGCAAGT TCAAAGGCACAGTC-3′ and 5′-CACCAGCATCACCCCATTT-3′ in the CFX96 Touch Real-Time PCR Detection System (Bio-Rad). GAPDH was used for normalization of RNA expression level.

Cell Viability Assay

Killing assays of CT-2A, GL261, and NXS2 were performed in 96-well plates (20,000 cells/well) using SFV4miRT or SFV4B18RmiRT in a gradient ranging from 0.01 to 10 MOI. Infection was performed either in the presence or absence of exogenous mIFN-β (5, 10, or 500 pg/mL). All treatments were performed in triplicates. Cell viability was assessed 2 to 3 days p.i. by measuring fluorescence of alamarBlue cell viability reagent (Thermo Fisher Scientific) at 585 nm after excitation at 570 nm in a Wallac 1420 VICTOR2 microplate reader (PerkinElmer, Turku, Finland). Relative viability (RV) was calculated by dividing fluorescence of transduced cells with that of the uninfected control

$$RV = \frac{FL(Transduced) - FL(Medium)}{FL(Untransduced) - FL(Medium)} x100.$$

Animal Experiments

All mice were housed at the BMC animal facility (Uppsala University) and the regional ethical committee has approved the use of animals for this study (ethical permit N164/15; N185/16).

CT-2A/fLuc tumor cells (40,000 in 2 μL) were implanted in the brain of female C57BL/6NRj mice (6 weeks) (Janvier labs, France). Tumor growth was monitored by measuring luminescence. Mice were treated by i.p. injection of PBS (n = 5) SFV4miRT (n = 8), or SFV4B18RmiRT (n = 8) (1×10^7 PFU in 100 μL PBS/mouse) 11 days post tumor inoculation. After viral infection, mice were monitored and neurological symptoms were scored: 0 = no symptoms; 0.1 = mild symptoms (mild limping, optic neuritis, and decreased activity); and 0.2–0.3 = combination of two or three 0.1 criteria, respectively, or severe symptoms expressed as paralysis. Mice were sacrificed when reaching a score of 0.3 and their brains were excised. A few mice were injected with the same amount of SFV4miRT (n = 3) and were sacrificed at an early time point to be able to compare to the mice infected with SFV4B18RmiRT sacrificed due to virus-related symptoms.

The right half of the brain containing the tumor was either snap frozen in methyl butane or embedded in paraffin after formaldehyde fixation and used for immunohistochemistry (IHC). The left tumor-free part of the brain was snap frozen and used for RNA extraction. Snap-frozen brain samples were thawed and homogenized in PBS using the Minilys personal homogenizer (Bertin, Rockville, MD). Homogenates were used to extract RNA using the RNeasy Plus Universal kit (QIAGEN). cDNAs were synthesized (iScript cDNA synthesis, Bio-Rad), SFV (nsP3), B18R, and miRTs were amplified using Phusion High-Fidelity DNA Polymerase (same primers as in qPCR), and SFV4-2SG-VVWB18R-miRT and irrelevant plasmids were used as positive and negative controls, respectively.

Immunohistochemical Analysis

Sections (6 μM) were prepared using a microtome and deparaffinized in Xylene, 100% EtOH, 95% EtOH, and 70% EtOH. Antigen was retrieved by boiling samples at 120°C in antigen unmasking solution (Vector Laboratories, Burlingame, CA) for 20 min. Endogenous peroxidases were blocked using 0.3% hydrogen peroxidase in methanol. After blocking with goat serum (1:50 in PBS) for 1 hr, sections were stained using polyclonal rabbit anti-SFV antibody (1:4,000 in PBS) against SFV structural proteins (kind gift from Dr. Ari Hinkkanen, University of Eastern Finland). Slides were incubated with goat

anti-rabbit IgG horseradish peroxidase (HRP) antibody (G21234, Thermo Fisher Scientific) (1:1,000 in PBS) for 30 min, after which the ImmPACT DAB Peroxidase (HRP) Substrate (Cat: SK-4105, Vector Laboratories, Burlingame, CA) was added to visualize the antibody staining. Then, the sections were counter stained with hematoxylin for 3 min, dehydrated, and mounted. Pictures were acquired with AxioImager (ZEISS, Germany).

Plaque Assay

Plaque forming capacity of SFV4miRT and SFV4B18RmiRT was compared in a monolayer of NXS2 cells in the presence or absence of exogenous mouse IFN-β (mIFN-β) (10 pg/mL). In a 6-well plate, 5×10^5 cells were plated 2 days before infection. Cells were infected at MOI 0.005 in 500 μL culture medium for 1 hr at 37°C. Infectious medium was replaced with 2 mL culturing medium (with 2% FBS) containing 2% carboxymethyl cellulose, with or without mIFN-β. After 3 days, plaques were visualized using Crystal Violet and the plaque area (mm^2) was calculated using ImageJ.

Western Blot

CT-2A cells were infected with SFV4miRT or SFVB18RmiRT cells at MOI 10 for 6 hr. After 6 hr, virus-infected cells were incubated with or without exogenous mIFN-β (50 pg/mL) for 30 min, after which they were harvested in 1XNuPAGE LDS Sample Buffer (Thermo Fisher Scientific) containing 1XNuPAGE Sample Reducing Agent (Thermo Fisher Scientific) on ice. Samples were boiled at 95°C for 10 min and resolved in a 4%–12% Bis-Tris Protein Gel (Thermo Fisher Scientific). Wet transfer was used to transmit proteins to a nitrocellulose membrane, which was blocked in 5% BSA in TBS-Tween (0.05%) for 2 hr. The membrane was probed with anti-p-STAT1 (Tyr701) (1:1,000 ab29045, Abcam, Cambridge, UK), targeting both p91 and p84 splice variants or β-actin antibody (A2228, Sigma) (1:10,000) in 3% BSA TBS-Tween (0.05%) at 4°C overnight. The membrane was probed with secondary antibody conjugated to HRP (1:1,000 in TBS-Tween) for 1 hr, after which the proteins were detected using the Amersham ECL Western Blotting Detection Kit (GE Healthcare, Uppsala, Sweden) in the ChemiDoc Touch imaging system (Bio-Rad). To determine the neutralizing effect of B18R, BHK21 cells were infected with SFV4miRT or SFV4B18RmiRT at MOI 10 and incubated overnight. Supernatants, containing secreted B18R, were collected from uninfected and virus-infected cells, and samples were either left untreated or treated with exogenous mIFN-β (200 pg/mL) for 1 hr. Supernatants were then applied to CT-2A cells for 30 min, after which cells were collected for western blot analysis to detect p-STAT1. Western blot was performed as described above. The amount of pSTAT-1 (both isoforms) was normalized to β-actin using ImageLab 5.0 (Bio-Rad).

ELISA

CT-2A cells were infected with SFV4miRT or SFV4B18RmiRT at MOI 10 overnight. Supernatants were collected and used for mIFN-β detection. ELISA was performed using the LEGEND MAX Mouse IFN-β ELISA Kit (BioLegend, San Diego, CA) according to the manufacturer's protocol.

Statistical Analysis

One-way ANOVA with either Tukey or Sidak post hoc test were used to compare means between more than two experimental groups. Oncolytic capacity and tumor growth were compared using two-way ANOVA with Holm-Sidak and Tukey post hoc tests, respectively. A p value less than 0.05 was considered as statistically significant.

SUPPLEMENTAL INFORMATION

Supplemental Information includes two figures and can be found with this article online at https://doi.org/10.1016/j.omto.2017.10.001.

AUTHOR CONTRIBUTIONS

Conception and Design, T.S., M.R., M.M., D.Y.; Acquisition of Data, T.S., M.R., D.Y.; Analysis and Interpretation of Data: T.S., M.R.; Writing, Review, and/or Revision of the Manuscript: T.S., M.R., M.M., D.Y.

CONFLICTS OF INTEREST

The authors declare no financial conflict of interest.

ACKNOWLEDGMENTS

The authors thank Prof. Magnus Essand (Uppsala University) for valuable discussion; Jing Ma (Uppsala University) for assistance in molecular cloning; Minttu-Maria Martikainen (Uppsala University) for assistance with in vivo work; and BioVis (Science for Life laboratory, Uppsala University) for imaging service.

REFERENCES

1. Alifieris, C., and Trafalis, D.T. (2015). Glioblastoma multiforme: pathogenesis and treatment. Pharmacol. Ther. *152*, 63–82.
2. Furnari, F.B., Fenton, T., Bachoo, R.M., Mukasa, A., Stommel, J.M., Stegh, A., Hahn, W.C., Ligon, K.L., Louis, D.N., Brennan, C., et al. (2007). Malignant astrocytic glioma: genetics, biology, and paths to treatment. Genes Dev. *21*, 2683–2710.
3. Ostrom, Q.T., Gittleman, H., Fulop, J., Liu, M., Blanda, R., Kromer, C., Wolinsky, Y., Kruchko, C., and Barnholtz-Sloan, J.S. (2015). CBTRUS statistical report: primary brain and central nervous system tumors diagnosed in the United States in 2008-2012. Neuro. Oncol. *17* (*Suppl 4*), iv1–iv62.
4. Kaufman, H.L., Kohlhapp, F.J., and Zloza, A. (2015). Oncolytic viruses: a new class of immunotherapy drugs. Nat. Rev. Drug Discov. *14*, 642–662.
5. Fazakerley, J.K. (2002). Pathogenesis of Semliki Forest virus encephalitis. J. Neurovirol. *8* (*Suppl 2*), 66–74.
6. Martikainen, M., Niittykoski, M., von und zu Fraunberg, M., Immonen, A., Koponen, S., van Geenen, M., Vähä-Koskela, M., Ylösmäki, E., Jääskeläinen, J.E., Saksela, K., et al. (2015). MicroRNA-attenuated clone of virulent Semliki Forest virus overcomes antiviral type i interferon in resistant mouse CT-2A glioma. J. Virol. *89*, 10637–10647.
7. Heikkilä, J.E., Vähä-Koskela, M.J., Ruotsalainen, J.J., Martikainen, M.W., Stanford, M.M., McCart, J.A., Bell, J.C., and Hinkkanen, A.E. (2010). Intravenously administered alphavirus vector VA7 eradicates orthotopic human glioma xenografts in nude mice. PLoS One *5*, e8603.
8. Ramachandran, M., Yu, D., Dyczynski, M., Baskaran, S., Zhang, L., Lulla, A., Lulla, V., Saul, S., Nelander, S., Dimberg, A., et al. (2016). Safe and effective treatment of experimental neuroblastoma and glioblastoma using systemically delivered triple microRNA-detargeted oncolytic Semliki Forest virus. Clin. Cancer Res. *23*, 1519–1530.
9. Ruotsalainen, J., Martikainen, M., Niittykoski, M., Huhtala, T., Aaltonen, T., Heikkilä, J., Bell, J., Vähä-Koskela, M., and Hinkkanen, A. (2012). Interferon-β sensitivity of

tumor cells correlates with poor response to VA7 virotherapy in mouse glioma models. Mol. Ther. *20*, 1529–1539.

10. Ruotsalainen, J.J., Kaikkonen, M.U., Niittykoski, M., Martikainen, M.W., Lemay, C.G., Cox, J., De Silva, N.S., Kus, A., Falls, T.J., Diallo, J.S., et al. (2015). Clonal variation in interferon response determines the outcome of oncolytic virotherapy in mouse CT26 colon carcinoma model. Gene Ther. *22*, 65–75.
11. Ylösmäki, E., Martikainen, M., Hinkkanen, A., and Saksela, K. (2013). Attenuation of Semliki Forest virus neurovirulence by microRNA-mediated detargeting. J. Virol. *87*, 335–344.
12. McNab, F., Mayer-Barber, K., Sher, A., Wack, A., and O'Garra, A. (2015). Type I interferons in infectious disease. Nat. Rev. Immunol. *15*, 87–103.
13. Sadler, A.J., and Williams, B.R. (2008). Interferon-inducible antiviral effectors. Nat. Rev. Immunol. *8*, 559–568.
14. Symons, J.A., Alcamí, A., and Smith, G.L. (1995). Vaccinia virus encodes a soluble type I interferon receptor of novel structure and broad species specificity. Cell *81*, 551–560.
15. Colamonici, O.R., Domanski, P., Sweitzer, S.M., Larner, A., and Buller, R.M. (1995). Vaccinia virus B18R gene encodes a type I interferon-binding protein that blocks interferon alpha transmembrane signaling. J. Biol. Chem. *270*, 15974–15978.
16. Alcamí, A., Symons, J.A., and Smith, G.L. (2000). The vaccinia virus soluble alpha/beta interferon (IFN) receptor binds to the cell surface and protects cells from the antiviral effects of IFN. J. Virol. *74*, 11230–11239.
17. Le Boeuf, F., Diallo, J.S., McCart, J.A., Thorne, S., Falls, T., Stanford, M., Kanji, F., Auer, R., Brown, C.W., Lichty, B.D., et al. (2010). Synergistic interaction between oncolytic viruses augments tumor killing. Mol. Ther. *18*, 888–895.
18. Dai, P., Wang, W., Yang, N., Serna-Tamayo, C., Ricca, J.M., Zamarin, D., Shuman, S., Merghoub, T., Wolchok, J.D., and Deng, L. (2017). Intratumoral delivery of inactivated modified vaccinia virus Ankara (iMVA) induces systemic antitumor immunity via STING and Batf3-dependent dendritic cells. Sci. Immunol. *2*, eaal1713.
19. Vähä-Koskela, M.J., Le Boeuf, F., Lemay, C., De Silva, N., Diallo, J.S., Cox, J., Becker, M., Choi, Y., Ananth, A., Sellers, C., et al. (2013). Resistance to two heterologous neurotropic oncolytic viruses, Semliki Forest virus and vaccinia virus, in experimental glioma. J. Virol. *87*, 2363–2366.
20. Fragkoudis, R., Tamberg, N., Siu, R., Kiiver, K., Kohl, A., Merits, A., and Fazakerley, J.K. (2009). Neurons and oligodendrocytes in the mouse brain differ in their ability to replicate Semliki Forest virus. J. Neurovirol. *15*, 57–70.
21. Le Bœuf, F., Batenchuk, C., Vähä-Koskela, M., Breton, S., Roy, D., Lemay, C., Cox, J., Abdelbary, H., Falls, T., Waghray, G., et al. (2013). Model-based rational design of an oncolytic virus with improved therapeutic potential. Nat. Commun. *4*, 1974.
22. Cronin, M., Le Boeuf, F., Murphy, C., Roy, D.G., Falls, T., Bell, J.C., and Tangney, M. (2014). Bacterial-mediated knockdown of tumor resistance to an oncolytic virus enhances therapy. Mol. Ther. *22*, 1188–1197.
23. Fragkoudis, R., Breakwell, L., McKimmie, C., Boyd, A., Barry, G., Kohl, A., Merits, A., and Fazakerley, J.K. (2007). The type I interferon system protects mice from Semliki Forest virus by preventing widespread virus dissemination in extraneural tissues, but does not mediate the restricted replication of avirulent virus in central nervous system neurons. J. Gen. Virol. *88*, 3373–3384.
24. Fu, X., Rivera, A., Tao, L., and Zhang, X. (2012). Incorporation of the B18R gene of vaccinia virus into an oncolytic herpes simplex virus improves antitumor activity. Mol. Ther. *20*, 1871–1881.